# Improving Beam Management Signalling for 5G NR Systems using Hybrid Beamforming

Fernandes, Filipa Santana da Silva; Rom, Christian; Harrebek, Johannes; Manchon, Carles Navarro

*Published in:*
2022 IEEE Wireless Communications and Networking Conference (WCNC)

*DOI (link to publication from Publisher):*
10.1109/WCNC51071.2022.9771993

*Publication date:*
2022

*Document Version*
Accepted author manuscript, peer reviewed version

# Improving Beam Management Signalling for 5G NR Systems using Hybrid Beamforming

Filipa Fernandes*, Christian Rom†, Johannes Harrebek†, Carles Navarro Manchón*
* Department of Eletronic Systems, Aalborg University, Denmark
Email: {fsdsf, cnm}@es.aau.dk
† Nokia Bell Labs, Aalborg, Denmark
Email: {christian.rom, johannes.harrebek}@nokia-bell-labs.com

***Abstract*—5th Generation (5G) millimeter wave (mmWave) communications are enabled through directive and narrow beams that mitigate these frequencies' challenging propagation conditions. In the future, 5G-Advanced and 6G will go even higher in the frequency spectrum, to allow for progressively larger bandwidths. The need for a larger number of narrower beams will put a strain in the current analog beamforming (BF) based beam management (BM) framework. This paper proposes an alternative signalling method for BM to parallelize the beam sweeping procedure using a hybrid analog-digital (HAD) BF architecture to enable mmWave signal multiplexing with a manageable overhead. The proposed solution is shown to significantly enhance beam alignment performance while reducing signalling overhead and latency.**

***Index Terms*—5G NR, beam management, mmWave, hybrid beamforming, beam tracking.**

## I. Introduction

The 5th Generation (5G) new radio (NR) standard supports a range of next generation node base station (gNodeB) antenna architectures for different frequencies of operation, mainly based on the number of transceiver units (TXRU) that these technologies require. Given the poor propagation conditions at millimeter wave (mmWave) frequencies, large antenna arrays are required but the number of TXRU are not easily scalable. Large bandwidths, characteristic of mmWave, combined with bit resolution requirements makes them a high cost, complexity and power consuming solution. Therefore, fully digital architectures are typically reserved for the lower end of the 5G spectrum [1]. Instead, analog architectures are used for higher frequencies, to avoid the complexity-cost challenges of fully digital beamforming (BF). However, a single TXRU configuration comes with limitations such as the inability to multiplex signals in the spatial dimension.

In the current 5G standard, mmWave communications rely on beam-based operations [1]. This, along with the need for highly directional beams at the receiver and transmitter, prompt the issue of beam alignment that drives beam management (BM). This procedure can be described as a set of layer 1 (L1) and layer 2 operations that establish and maintain an optimal beam pair between the gNodeB and the user equipment (UE), thus ensuring adequate link quality while the UE moves through the cell [2]. Given the importance of this procedure, optimization of BM performance has been extensively pursued in the literature. In [3], a dynamic weight-based algorithm is proposed for initial access (IA) synchronization signal block (SSB) allocation, using static user distribution, to optimize the number of SSBs per sweeping direction. The authors in [4] introduce different beam switching algorithms to improve robustness of BM operations for intra-cell mobility scenarios. A mmWave IA protocol is developed in [5], with a compressive-sensing beam sweeping algorithm that achieves high BF gain, low misdetection probability and reduced search time. Furthermore, [6] employs a machine learning approach with a deep neural network trained for beam selection using reference signal received power (RSRP) measurements from standard compliant uplink signals in a high speed train use case, reducing signalling overhead and latency.

Most of these solutions still assume an analog architecture at the gNodeB array for BM. While the standard BM procedure performs adequately for current antenna array configurations, its ability to scale well in future cellular systems, where higher frequencies will be employed, is questionable. Larger antenna arrays will be required to compensate for the high frequency pathloss, making the beams even narrower. To maintain proper coverage, larger codebooks will need to be adopted, which will increase BM overhead, latency and overall complexity [7]. Therefore, the current BM framework must be updated to support a higher number of narrow beams. Hybrid BF architectures, which employ multiple radio frequency (RF) chains with analog phase shifters, can be used at mmWave as a compromise to enable spatial multiplexing while keeping a reduced number of TXRU and a manageable overhead [8].

This paper proposes a signalling scheme that enables the simultaneous transmission of spatially multiplexed SSBs for BM using low cross-correlation signals and a fully-connected hybrid analog-digital (HAD) architecture. Using Monte-Carlo simulations, it is shown that the proposed signalling scheme is able to reduce overhead and latency of the beam sweeping procedure while improving the overall beam alignment performance when compared to its currently standardized counterpart, particularly for high-speed scenarios.

The remainder of this paper is organized as follows: Section II describes the system model, while Section III presents the proposed signalling scheme. Section IV illustrates the performance of the proposed scheme and Section V concludes the paper and elaborates on future work.

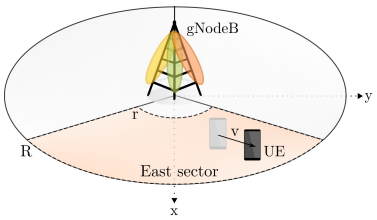


Fig. 1. Network layout.

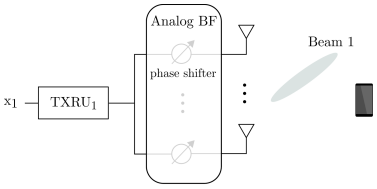


(a)

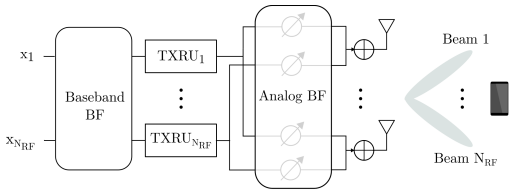


(b)

Fig. 2. BF architectures. (a) Analog array. (b) HAD fully-connected array.

## II. System Model

### A. Network Layout

A downlink (DL) single-cell mmWave system is considered, where the gNodeB attempts to achieve beam alignment with a moving UE. A tri-sector cell is assumed, as seen in Fig. 1, where the UE moves in a linear trajectory with a random direction at speed $v$ in the east sector, bound by mobility ranges $r$ and $R$. The gNodeB antenna array, standing at height $h_{TX}$ m, is equipped with a uniform linear array (ULA) panel of patch antennas of size $N_{TX}$. The UE is modeled as a single isotropic antenna, $N_{RX} = 1$, at a height of $h_{RX}$ m[1].

### B. Signal Model

During the beam sweeping stage of BM, the gNodeB transmits several SSBs to determine the best beam to serve each UE. BF is undertaken with an analog or a HAD fully-connected architecture using $N_{RF}$ TXRU, as seen in Fig. 2 (a) and Fig. 2 (b), respectively.

The generalized expression for the UE received signal at time-frequency resource $k$ is given by

$$y(k) = \boldsymbol{h}(k)^\top \boldsymbol{F}(k)\boldsymbol{x}(k) + n(k) \tag{1}$$

where $\boldsymbol{h}(k) \in \mathbb{C}^{N_{TX}}$ is the DL channel vector between the UE and the gNodeB in the $k$th time-frequency resource. These channel coefficients are obtained through a 3D geometry-based stochastic channel model generator, QuaDRiGa, which is compliant with current 3rd generation partnership project (3GPP) standards for channel modelling [9]. In the gNodeB BF matrix $\boldsymbol{F}(k) \in \mathbb{C}^{N_{TX} \times N_{RF}}$, each column contains the analog phase shifts $\boldsymbol{f}_b \in \mathbb{C}^{N_{RF}}$ for a beam $b$ used by a TXRU to transmit an SSB symbol in the $k$th time-frequency resource. Due to the analog implementation, all entries of $\boldsymbol{F}(k)$ have a constant modulus of $\frac{1}{\sqrt{N_{TX}}}$. The vector $\boldsymbol{x}(k) \in \mathbb{C}^{N_{RF}}$ expresses the $N_{RF}$ transmitted SSB symbols in the $k$th time-frequency resource, with a symbol variance of $\frac{1}{\sqrt{N_{RF}}}$. This signal is generated using the 5G Toolbox™ from MATLAB® [10]. Finally, $n(k) \backsim \mathcal{CN}(0, \sigma^2)$ is the receiver's noise in the $k$th time-frequency resource modeled as a complex additive white Gaussian noise (AWGN) vector. This work assumes perfect subcarrier orthogonality conditions, specifically that the maximum channel delay response is within the cyclic prefix duration and the channel response is constant during a full orthogonal frequency-division multiplexing (OFDM) symbol.

### C. gNodeB BF Codebook

To perform SSB-based beam sweeping at the gNodeB, a directional BF codebook is adopted, which divides the cell's sector coverage area into separate angular regions. These beams are chosen from a predefined, finite set of $N_{SS}$ vectors $\mathcal{C} = \{\boldsymbol{f}_b | b = 1, \ldots, N_{SS}\}$ which is referred henceforth as the codebook. The $b$th vector of the codebook is chosen as the array steering vector for angle $\phi_b$, i.e.

$$\boldsymbol{f}_b = \frac{1}{\sqrt{N_{TX}}}[1, e^{-j\pi \sin\phi_b}, \ldots, e^{-j\pi(N_{TX}-1)\sin\phi_b}]^T. \tag{2}$$

The angle $\phi_b$ is the azimuth angle to which the $b$th beam is pointing, measured on the xy plane with respect to the x axis. The steering angles $\phi_b$, are linearly spaced within the angular range of the sector so that

$$\phi_b = -\frac{\pi}{3} + (b-1) \times \frac{2\pi}{3 \times (N_{SS}-1)}, b = 1, 2, \ldots, N_{SS}. \tag{3}$$

## III. Signalling scheme

This section presents the proposed signalling scheme for gNodeB beam selection and how it differs from the current scheme in the standard. SSBs, or SS/PBCH blocks, are generally used, among other NR signals, for measurement purposes to ensure proper beam alignment between the gNodeB and the UE. As described in [11], an SSB is grouped into 4 OFDM symbols in time and 240 subcarriers in frequency. It carries a primary synchronization signal (PSS) and secondary synchronization signal (SSS), for initial synchronization and cell/beam identification, respectively. These signals are pseudo random binary sequences with 127 m-sequence values. Additionally, a physical broadcast channel (PBCH) is included, associated with a demodulation reference signal (DMRS). A group of SSBs is identified as an SSBurst, where each SSB is mapped to a different gNodeB beam.

[1]This work focuses on the signalling from the gNodeB side and, as such, this simplifying assumption is taken. Extension of this proposal for multi-antenna UEs is straightforward.

### A. Current Scheme in 5G NR

In the current NR standard, the SSBurst lasts less than $5\,\mathrm{ms}$ and its periodicity $Tss$ varies from $5\,\mathrm{ms}$ to $160\,\mathrm{ms}$. All SSBs coming from a common gNodeB share the same PSS and SSS sequences, having the same cell ID. The maximum number of SSBs per SSBurst, $N_{max}$, as well as its resource mapping, are numerology-dependent [12]. For all numerologies, the SSB pattern always allocates one SSB at a time, as seen in Fig. 3 (a). The gNodeB performs analog beam sweeping with $Nss$ beams and the UE receives and decodes one SSB at a time. During this process, the signal will be sequentially correlated with known PSS and SSS sequences to recover the physical cell identity of the gNodeB. This information is used to process PBCH-DMRS resources which can be used, together with SSS, to measure L1-RSRP [13]. Finally, the UE stores a subset of the best $N$ RSRP values and reports them back to the gNodeB for beam determination. This study takes the current standardized scheme as a baseline to compare to the proposed scheme in terms of beam alignment performance.

### B. Proposed Scheme

The proposed scheme employs the capabilities of a fully-connected HAD BF architecture to transmit $N_{RF}$ SSBs in parallel while keeping the same array gain. To distinguish simultaneously transmitted SSBs, each of them must be associated with an unique PSS and SSS combination, exploiting the low cross-correlation nature of these sequences to preserve beam-specific information. Keeping the same SSBurst periodicity and block pattern, SSB groups are transmitted in overlapping time-frequency resources, creating $\frac{N_{SS}}{N_{RF}}$ transmission instances $t$. The best beam per group is identified during the PSS and SSS decoding stage. In each $t$, after recovering the correct PSS sequence, the UE searches the time-frequency resources where SSS is allocated, $\mathcal{K}_{SSS}$, to compute the correlation function between the SSS portion of the received signal, $y^t_{sss}$, and all the reference SSS sequences, $r_{sss,b}$, for each beam $b$ through

$$X^t_{corr}[b] = \frac{1}{|\mathcal{K}_{SSS}|}\left|\sum_{k\in\mathcal{K}_{SSS}} y^t_{sss}(k) r^*_{sss,b}(k)\right| \tag{4}$$

where $|\mathcal{K}_{SSS}|$ denotes the cardinality of set $\mathcal{K}_{SSS}$. The strongest correlation peak of each $t$ is stored and reported back to the gNodeB for beam determination. The resources occupied for beam alignment are reduced by $\frac{1}{N_{RF}}$, as represented in Fig. 3 (b). However, each parallel beam also experiences a scaling in power by the same factor.

### C. Scheme Comparison

In order to enable the proposed scheme as add-on to the current standard, some requirements must be met. First, the beams assigned to grouped SSBs must be spatially separated to avoid inter-beam interference caused by beam overlap. Their beam indexes, extracted from the codebook $\mathcal{C}$, should be separated by $\frac{N_{SS}}{N_{RF}}$ positions. Furthermore, the beam indexing information for beams of the same group should be mapped to their unique PSS and SSS combination. Therefore, the PSS and SSS sequences of a group must present low cross-correlation.

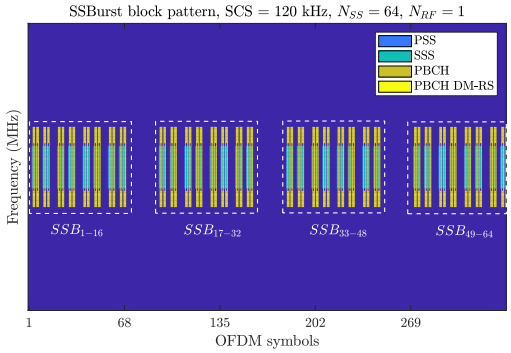


(a)

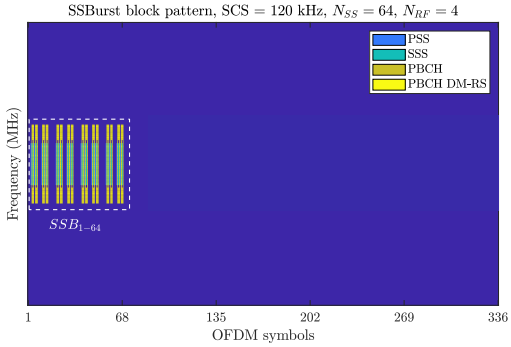


(b)

Fig. 3. SSBurst block pattern for $SCS = 120\,\mathrm{kHz}$, $T_{SS} = 20\,\mathrm{ms}$, $N_{SS} = 64$. (a) Current implementation. (b) Proposed implementation with $N_{RF} = 4$.

## IV. Results and Discussion

This section details the performance evaluation of the proposed scheme. The key performance indicators (KPIs) used are detailed in Subsection IV-A. Subsection IV-B showcases the overhead advantage of the proposed scheme while Subsection IV-C focuses on the latency benefits for high-speed scenarios. Table I summarizes all the simulation parameters used.

### A. KPIs

To evaluate beam alignment performance, received signal strength (RSS) measurements are performed over the time-frequency resources reserved for data transmission. This study assumes a potential data resource allocation set, $\mathcal{K}_{data}$, that occupies the whole available bandwidth $B$ and time interval between consecutive SSBursts, as displayed in Fig. 4 for a generic SSBurst set[2]. The transmission window of one SSBurst and one $\mathcal{K}_{data}$ set is referred to as a measurement period, $MP$, and lasts for $T_{SS}$ ms. The RSS over $\mathcal{K}_{data}$ for a beam $b$ is defined as

$$R[b] = \frac{1}{|\mathcal{K}_{data}|}\sum_{k\in\mathcal{K}_{data}} |\boldsymbol{h}(k)^\top \boldsymbol{f}_b|^2 \tag{5}$$

[2]In a multi-user scenario, the available resource pool needs to be shared among users, resulting in a scaling of the absolute maximum achievable rate per user.

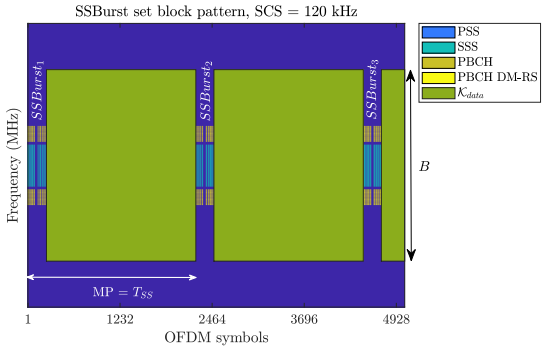


Fig. 4. Data time-frequency resource allocation.

where $|\mathcal{K}_{data}|$ denotes the cardinality of set $\mathcal{K}_{data}$, i.e., the amount of time-frequency resources available for data transmission. For the proposed approach, the best measured beam is dictated by the strongest SSS correlation peak over all different transmission instances $t$. The corresponding RSS is calculated as

$$R_{meas} = R[\arg\max_{b}(\max_{t} X^{t}_{corr}[b])]. \tag{6}$$

To evaluate beam selection accuracy, the measured RSS is compared to a genie beam selection. Considering optimal beam alignment, the maximum achievable RSS over all the $Nss$ available beams is determined by

$$R_{genie} = \max_{b} R[b]. \tag{7}$$

Misdetection probability is defined as the probability that the selected best beam does not correspond to the optimal beam, given by

$$P_m = \mathbb{P}[R_{meas} < R_{genie}]. \tag{8}$$

The impact of misdetections can vary, depending on how misaligned the measured beam is to the genie beam choice. Therefore, an additional criteria is introduced to quantify the beam misdetection loss, written as

$$\Delta SNR = \frac{R_{genie}}{R_{meas}}. \tag{9}$$

To differentiate which misdetections actually jeopardize communications, $P_{m,3dB}$ expresses the probability that the $\Delta SNR$ incurred exceeds 3 dB as

$$P_{m,3dB} = \mathbb{P}[\Delta SNR_{dB} \geq 3\,\mathrm{dB}]. \tag{10}$$

After beam alignment, the channel's maximum achievable spectral efficiency is calculated as

$$S = \log_2(1 + \frac{R_{meas}}{\sigma^2}). \tag{11}$$

TABLE I
SIMULATION PARAMETERS

| Parameter | Notation | Overhead Study | High-speed study |
|---|---|---|---|
| Carrier frequency | $f$ | 28 GHz | |
| Carrier Bandwidth | $B$ | 200 MHz | |
| sub-carrier spacing (SCS) | $SCS$ | 120 kHz | |
| Maximum SSBs / SSBurst | $N_{max}$ | 64 | |
| SSBurst periodicity | $T_{SS}$ | 20 ms | |
| Inner / Outer mobility bound | $r$ / $R$ | 15 m / 100 m | 15 m / 200 m |
| Channel model | - | UMi LOS | UMa LOS |
| gNodeB position | $(x, y)$ | $(0, 0)$ | |
| gNodeB height | $h_{TX}$ | 10 m | 25 m |
| gNodeB TX power | $P_{TX}$ | 30 dBm | |
| UE position | $(x, y)$ | random within east sector | |
| UE height | $h_{RX}$ | 1.5 m | |
| UE speed | $v$ | 60 km h$^{-1}$ | 120 km h$^{-1}$ |
| Number of UE trajectories | $N_{traj}$ | 2000 | |
| RX Noise Figure | $NF$ | 9 dB | |
| Thermal noise density | $N_0$ | $-174$ dBm Hz$^{-1}$ | |
| gNodeB / UE antenna element | - | patch [14] / isotropic | |
| gNodeB / UE array size | $N_{TX}$ / $N_{RX}$ | 64 / 1 | |

TABLE II
DETECTION ACCURACY

| $N_{ss}$ | $N_{RF}$ | $N_{TX}$ | $P_m$ [%] | $P_{m,3dB}$ [%] |
|---|---|---|---|---|
| 16 | 1 | 64 | 16.05 | 6.30 |
| | | 32 | 6.85 | 2.85 |
| | | 16 | 3.25 | 0.25 |
| 32 | 2 | 64 | 6.05 | 3.05 |
| 64 | 4 | 64 | 6.55 | 0.40 |

### B. Comparison of SSB Schemes with Common Overhead

With the proposed scheme, it is possible to support a larger gNodeB array codebook during BM without an overhead increase. This section compares the BM performance of a UE moving at 60 km h$^{-1}$ under three different SSB transmission schemes with equal overhead: $N_{SS} = 16$ with $N_{RF} = 1$, $N_{SS} = 32$ with $N_{RF} = 2$ and $N_{SS} = 64$ with $N_{RF} = 4$. Due to the large array size and reduced number of beams, the first SSB transmission scheme is also tested for two smaller array dimensions, to reduce coverage gaps with wider beams. Table II displays the $P_m$ and $P_{m,3dB}$ values for each scheme. From the $N_{TX} = 64$ results, it is clear that beam alignment performance improves with $N_{SS}$. Since the beams are very narrow, to keep a good coverage level, a larger codebook must be employed. With $N_{SS} = 64$ and $N_{RF} = 4$ it is possible to use four times more beams with the same overhead, which improves coverage significantly. This results in less misdetections, an improved signal-to-noise ratio (SNR) and consequently, enhanced spectral efficiency, as shown in Fig. 5 and Fig. 6. However, if the scheme comparison is repeated for $N_{SS} = 16$ with $N_{TX} = 16$, the $P_m$ from the schemes with $N_{RF} > 1$ become larger than the baseline. Since the array size is smaller, the beams lose gain and become wider, covering the sector uniformly. This approach reduces the maximum achievable spectral efficiency of this scheme but also decreases the number of beam misdetections. The increase in misdetections for the proposed scheme are due to inter-beam interference and

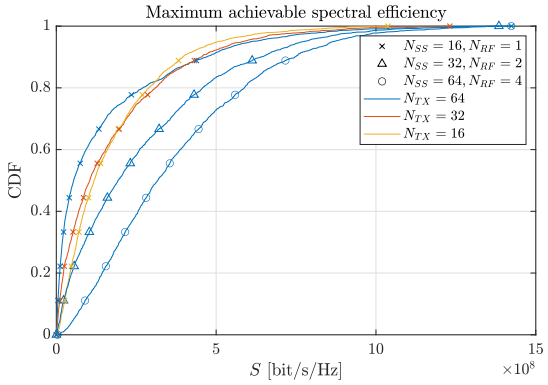


Fig. 5. Maximum achievable spectral efficiency for three SSB schemes with common overhead, UMi LOS, $v = 60\,\mathrm{km\,h^{-1}}$.

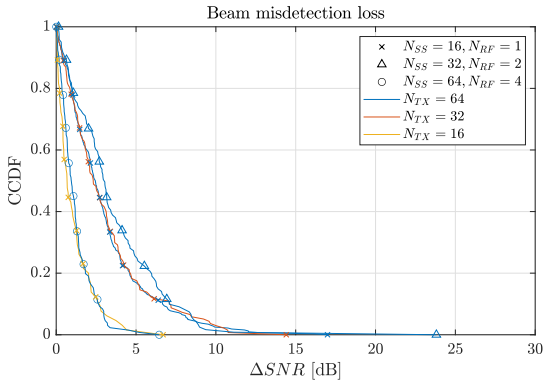


Fig. 6. Beam misdetection SNR loss for three SSB schemes with common overhead, UMi LOS, $v = 60\,\mathrm{km\,h^{-1}}$.

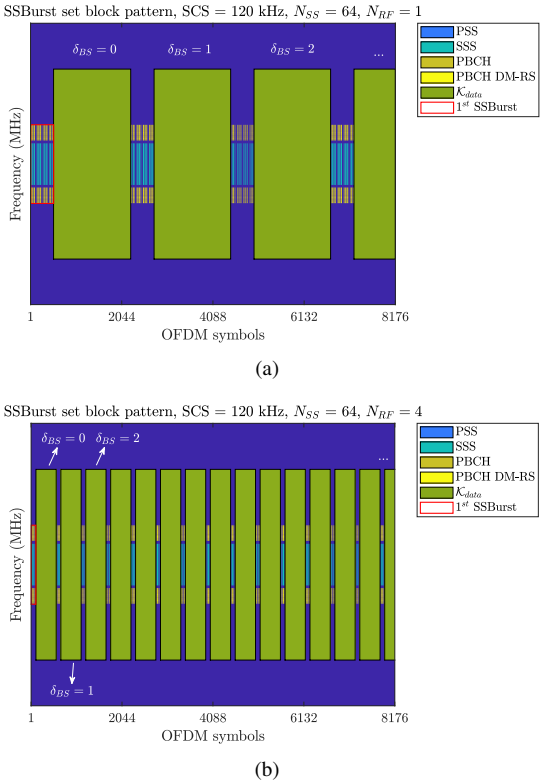


Fig. 7. Selected beam usage for data transmission with different beam selection delays. (a) baseline scheme: $N_{SS} = 64, N_{RF} = 1$. (b) proposed scheme: $N_{SS} = 64, N_{RF} = 4$.

reduced power levels per beam sent simultaneously. However, the performance of these schemes is still considerably higher compared to the baseline scheme in terms of misdetection loss and spectral efficiency, due to the larger overlap between beams which makes beam misalignment errors less significant. This is evident from the $P_{m,3dB}$ results in Table II. Although the number of misdetections is larger, the occurrences where the power loss incurred is large enough to deteriorate communications is greatly reduced, especially for larger codebooks. In conclusion, this signalling scheme may enable the use of larger amounts of beams to improve coverage without overhead or latency costs, provided that adequate beam separation and transmit power are provided.

### C. Scheme Performance for a High-Speed Scenario

So far, the UE measurement and reporting stage, as well as the gNodeB beam determination process have been considered to have a negligible delay. In reality, besides scheduling and processing delays, the UE may need to scan the gNodeB beams multiple times, either to smooth out fast fading effects or to measure different UE beams, assuming BF on the receiver side. This results in a delay of the beam selection operation. While those delays can be safely overlooked for low and moderate speeds, they can have a significant impact on beam alignment performance for high mobility UEs, since beam information becomes outdated faster. Fig. 7 (a) illustrates which $\mathcal{K}_{data}$ period would be the first to employ the beam selection obtained through the measurements collected in the first SSBurst (highlighted in red), for different values of beam selection delay, $\delta_{BS}$. If one $MP$ is considered as the smallest unit of $\delta_{BS}$, an instantaneous beam selection corresponds to $\delta_{BS} = 0$, where the first $\mathcal{K}_{data}$ is transmitted with the beam selected in the same $MP$. If the delay is now considered to be $\delta_{BS} = 1$, then the beam selected with the measurements from the first SSBurst will only be in effect one $MP$ later, in the second $\mathcal{K}_{data}$. With the proposed scheme, it is possible to keep the same overhead as in the baseline case and perform more frequent beam updates. Reducing the beam scan latency by a factor of $N_{RF}$ allows for an increased beam scan periodicity, as seen in Fig. 7 (b). It is assumed that the beam measurement, reporting and determination time constraints mentioned above can be equally compressed with the proposed scheme. The baseline signalling scheme is compared to the proposed scheme, at $v = 120\,\mathrm{km\,h^{-1}}$, for $\delta_{BS} = 0$, $\delta_{BS} = 1$ and $\delta_{BS} = 3$.

Results in Table III indicate that, as expected, $P_m$ becomes larger when $\delta_{BS}$ for the baseline scheme increases, due to high-speed channel variability. This leads to high misdetection loss which deteriorates the maximum achievable spectral efficiency, as shown in Fig. 8 and Fig. 9. Employing the proposed solution results in a decrease of $P_m$ which improves

TABLE III
DETECTION ACCURACY

| $N_{ss}$ | $N_{RF}$ | $\delta_{BS}$ | $P_m$ [%] | $P_{m,3dB}$ [%] |
|---|---|---|---|---|
| 64 | 1 | 0 | 6.45 | 0.23 |
| | | 1 | 17.35 | 2.27 |
| | | 3 | 37.00 | 9.05 |
| 64 | 4 | 0 | 2.00 | 0.03 |
| | | 1 | 5.15 | 0.12 |
| | | 3 | 9.85 | 0.80 |

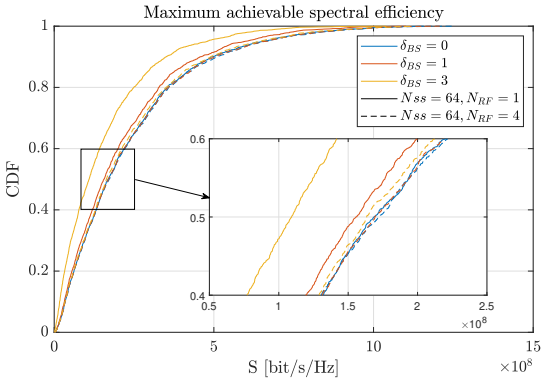


Fig. 8. Maximum achievable spectral efficiency comparison for the baseline and proposed schemes with different beam selection delays, UMa LOS, $v = 120\,\mathrm{km\,h^{-1}}$.

misdetection losses and achievable spectral efficiency. The $\delta_{BS}$ curves come close to the baseline scheme curve for $\delta_{BS} = 0$. It is worth mentioning that, although improvements for smaller values of $\delta_{BS}$ are less significant, this scheme is successful in improving speed robustness for BM without increased signalling for lower speeds.

## V. CONCLUSIONS

This paper proposes an alternative SSB transmission scheme for BM using low cross-correlation signalling and HAD BF in order to improve narrow beam alignment performance with a reduced amount of time-frequency resources. Results show that, with proper beam separation and power levels per beam, this proposal offers a significant improvement of beam detection accuracy and beam sweeping latency without requiring any additional overhead.

This work is meant to be a first step towards evolving the current BM procedure to support the overhead, latency and complexity challenges of future 5G and 6G signalling frameworks for larger antenna arrays. At higher frequencies, cellular systems will require larger BF gains but will also suffer the effects of reduced beamwidths. To guarantee coverage for all users, larger antenna arrays and codebooks will be indispensable. This scheme proposal would enable large codebook sizes of high-gain beams by scaling the signalling required to manage them, all while freeing up resources to improve the system's spectral efficiency. Although HAD BF consumes more energy due to the increase of TXRU, this solution is proposed to be employed on the gNodeB side, where the power cost constraints are less stringent. It boosts considerably the beam alignment performance with a reduced complexity and power consumption when compared to a fully-digital BF architecture. Moreover, to bring the proposed concept to practice, its interaction with time-frequency synchronization procedures will need to be considered, especially for high speed scenarios where perfect orthogonality assumptions may fall short for proper data decoding; this will be a subject of future research.

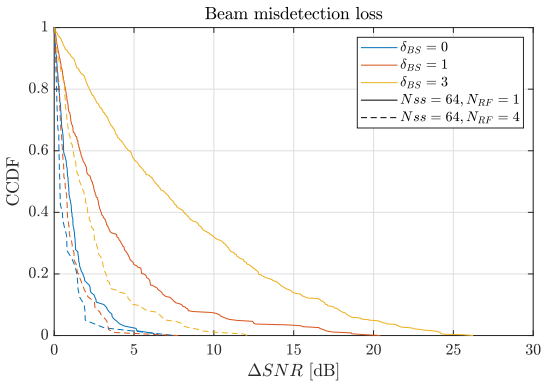


Fig. 9. Beam misdetection SNR loss comparison for the baseline and proposed schemes with different beam selection delays, UMa LOS, $v = 120\,\mathrm{km\,h^{-1}}$.

## REFERENCES


[1] M. Enescu *"5G New Radio: A Beam-based Air Interface"*, Wiley 2020.
[2] "Study on New Radio Access Technology - Physical Layer Aspects - Release 14", 3GPP, Sophia Antipolis, France, Rep TR 38.802, 2017.
[3] A. Indika Perera, K. B. Shashika Manosha, N. Rajatheva and Matti Latva-aho, "An Initial Access Optimization Algorithm for millimeter Wave 5G NR Networks", *2020 IEEE 91st Vehicular Technology Conference (VTC2020-Spring)*, Antwerp, Belgium, May 2020.
[4] U. B. Elmali, A. Awada, U. Karabulut and I. Viering, "Analysis and Performance of Beam Management in 5G Networks", *2019 IEEE 30th Annual International Symposium on Personal, Indoor and Mobile Radio Communications (PIMRC)*, Istanbul, Turkey, September 2019.
[5] I. Aykin and M. Krunz, "Efficient Beam Sweeping Algorithms and Initial Access Protocols for Millimeter-Wave Networks", *IEEE Transactions on Wireless Communications*, vol. 19, no. 4, pp. 2504-2514, April 2020.
[6] Y. G. Lim, H. J. Ji, J. H. Park and Y. S. Kim, "Artificial Intelligence-Based Beam Management for High Speed Applications in mmWave Spectrum", *2020 IEEE Globecom Workshops (GC Wkshps)*, Taipei, Taiwan, December 2020.
[7] Y. Heng, *et al.*, "Six Key Challenges for Beam Management in 5.5G and 6G Systems", *IEEE Communications Magazine*, vol. 59, no. 7, pp. 74-79, July 2021.
[8] H. Yan, S. Ramesh, T. Gallagher, C. Ling and D. Cabric, "Performance, Power, and Area Design Trade-Offs in Millimeter-Wave Transmitter Beamforming Architectures", *IEEE Circuits and Systems Magazine*, vol. 19, no. 2, 2019.
[9] S. Jaeckel, L. Raschkowski, K. Börner and L. Thiele, "QuaDRiGa: A 3-D Multicell Channel Model with Time Evolution for Enabling Virtual Field Trials", *IEEE Transactions on Antennas Propagation*, vol. 62, pp. 3242 - 3256, 2014.
[10] MathWorks, *5G Toolbox*, Natick Massachusetts, US, 2019.
[11] *5G NR - Physical channels and modulation - Release 15*, 3GPP Standard TS 38.211, 2018.
[12] *NR - Physical layer procedures for control - Release 15*, 3GPP Standard TS 38.213, 2019.
[13] *NR - Physical layer measurements - Release 15*, 3GPP Standard TS 38.215, 2019.
[14] "Study on channel model for frequencies from 0.5 to 100 GHz - Release 15", 3GPP, Sophia Antipolis, France, Rep TR 38.901, 2018.